HHS Public Access

Author manuscript

J Surg Res (Houst). Author manuscript; available in PMC 2022 August 05.

Published in final edited form as:

J Surg Res (Houst). 2022 ; 5(3): 423–434. doi:10.26502/jsr.10020237.

Heterogeneous Population of Immune cells Associated with Early Thrombosis in Arteriovenous Fistula

Gunimat Samra,

Vikrant Rai,

Devendra K. Agrawal*

Department of Translational Research, Western University of Health Sciences, Pomona CA 91766, USA

Abstract

End-Stage Renal Disease (ESRD) is a growing cause of morbidity and mortality in the practice of modern medicine. Advances in medicine have elongated the average life span and subsequently made chronic diseases prevalent. Hemodialysis is the main treatment that is used to treat ESRD and is a clinical procedure that is being re-imagined with novel approaches to improve patient and clinic practicality and effectiveness. Arteriovenous Fistulas (AVF) are now used in place of catheters due to their higher success and lower co-morbidities. The main drawback of AVF is the time gap that is needed from the surgical creation of AVF to its use. During this time, the AVF is susceptible to thrombosis and occlusion rendering the fistula ineffective for treatment. Immune cells play a major role in vascular pathologies and macrophages, dendritic cells, and T-regulatory cells are the main cells seen during the inflammatory and anti-inflammatory phases. However, the role of immune response and immune cells in AVF maturation is poorly understood. This study aimed to investigate the immune response and immune cell expression in femoral vessels after AVF creation in a miniswine model of AVF using immunohistochemistry and qRT-PCR. The results of this study revealed an increased expression of immune cells in AVF vessels and suggest an association of immune response with AVF creation and maturation.

Keywords

Arteriovenous Fistula; AVF maturation; Immune response; Immune cells; Inflammation

Introduction

Arteriovenous fistula (AVF) is an abnormal connection between artery and vein utilized by surgeons and clinicians to gain access to the arterial and venous arms for hemodialysis. AVF is currently used primarily in patients that are treated for End-Stage Renal Disease

***Corresponding author:** Devendra K. Agrawal, Department of Translational Research, Western University of Health Sciences, Pomona CA 91766, USA.

Conflict of interest

As the corresponding author, I declare that this manuscript is original; that the article does not infringe upon any copyright or other proprietary rights of any third party; that neither the text nor the data have been reported or published previously. All the authors have no conflict of interest and have read the journal's authorship statement.

(ESRD) with dialysis. Treatment for ESRD via hemodialysis was initially implemented using catheters and vein grafts, however, risks of disease and complications with managing catheters and grafts have made them obsolete to this newfound procedure [1,2]. AVF is a suitable procedure with fewer risks of disease and complications in the management of hemodialysis. Although AVF is now the primary tool to perform hemodialysis, they come with its own sets of limitations. There is no universal definition for a mature AVF, however, the National Kidney Foundation's Kidney Disease Outcomes Quality Initiative (NFK-KDOQI) has set guidelines that introduce 'the rule of 6' to define maturation in humans. Maturation with the rule of 6 is defined as a flow of 600 ml/min, AVF depth of <6 millimeters from the skin surface, and a minimum diameter of 6 millimeters [3]. This healing process takes at least 12 weeks to fully mature before AVF can be utilized for dialysis treatment [3]. During the healing process, the AVF can fail and become completely thrombosed leading to early AVF failure. The created fistula with thrombosis can no longer be used to perform hemodialysis resulting in poor patient prognosis and excessive cost for the patient and hospital. The high incidence of non-maturation in AVF is the main drawback that must be addressed to advance this lifesaving treatment for a superior patient-treatment outcome. Multiple factors contribute to AVF failure including the surgeon performing the surgery and the individualized patient factors. Known factors that are linked with an increased rate of AVF failure are age, sex, and diabetes mellitus [3]. Hemodynamics changes, immune cell aggregation, and inflammatory response of the patient lead to remodeling of the vessel and contribute individually to the fate of AVF [4]. The sheer wall stress experienced by the endothelium leads to vascular remodeling and thickening of the intima leading to generalized thickening and outward remodeling of the outflow vessel [5]. This thickening is necessary for the full maturation of AVF, however, if it continues and goes unchecked by the immune response, it can result in stenosis or complete occlusion due to thrombosis, and thus failing the AVF [3,4]. The creation of AVF and maturation is involved in an intricate balance between pro-inflammatory and anti-inflammatory endogenous responses [5]. Since persistent inflammation is involved in early thrombosis of involved vessels, targeting immune response and inflammation may play a therapeutic role during the early and late phases of inflammation and AVF maturation [6]. Additionally, regulation of early arterial thrombosis with genetic and epigenetic factors in association with the involvement of immune cells supports the role of immune regulation of AVF maturation and maturation failure [7]. Crosstalk of inflammatory and anti-inflammatory mediators with immune cells contributes to the outcome of AVF development [8]. Mediators such as damage-associated molecular patterns (DAMPs), the receptor for advanced glycation end products (RAGE), high-mobility group box protein (HMGB)-1, nuclear factor kappa beta (NF-κB), interleukin (IL)-1, IL-6, IL-10, and IL-12 contribute uniquely to alter the phenotypic behavior of immune response in the developing AVF [9-11]. These receptors, cytokines, and secondary messengers are integrated through key immune cells that alter the microenvironment of the AVF site. Macrophages, dendritic cells (DC), and T cells morph between the inflammatory and anti-inflammatory spectrum to influence the surrounding environment and promote healing. Post-operative surgery, dissected tissue, and surgical wounds heal through phases of inflammation; however, the persistence of chronic inflammation may result in fibrosis of surrounding tissue and thrombosis of the vessel [6]. Further, the presence of molecular mechanisms related to immune cells on

transcriptomic analysis with early thrombosis supports the role of immune cells in AVF maturation and failure [7]. In this study, we hypothesized that chronicity of inflammation causes early thrombosis of the vessels and investigated the presence, characteristics, and proportion of inflammatory and anti-inflammatory immune cells in AVF vessels in swine models using known surface markers. The results of this study revealed an association of innate and adaptive immune response with early AVF thrombosis and the proportion of pro-and anti-inflammatory immune cells in AVF vessels. Targeting immune response and regulating the proportion of pro-and anti-inflammatory immune cells may be of therapeutic significance in the prevention of early thrombosis.

Materials and Methods

Animal Model

We recently reported the procedure and the characteristics of the animal model used in this study [6]. Briefly, Yucatan miniswine purchased from Premier Bio-Resource (Ramona, California) weighing approximately 20-30 kg were kept at a 12-hour light-dark cycle with a temperature ranging from 72-74°F and used for this study. The miniswine were fed Mini-Pig Grower Diet (Test Diet # 5801) with water *ad libitum* and housed at the animal facility at Western University of Health and Science, Pomona, CA. Only female swine were used due to ease of handling and more importantly the avoidance of potential confounding factors due to castration of male swine. The vessels collected from 16 pigs from four experimental groups including (i) 30% ethanol (n=4), (ii) ethanol + TAK242 (n=4), (iii) LR12 peptide (n=4), and (iv) scrambled peptide (n=4, SP), were used in this study. All animal experiments and interventions were approved by the institutional animal care and use committee (IACUC, approval # R20IACUC038) of Western University of Health Sciences, Pomona, CA The expression of the cells was compared between the LR12 peptide (triggering receptor expressed on myeloid cells (TREM-1) inhibitor)-treated and scrambled peptide (SP)-treated groups. Similarly, the TAK-242 (a specific inhibitor of toll-like receptor (TLR)-4) treated group was compared with the vehicle (30% ethanol)-treated group. In an ongoing research protocol in our laboratory, the inhibition of TLR-4 via TAK 242 and TREM 1 via LR12 was used to suppress the downstream effects of these inflammatory cascades [12-14] to attenuate inflammation. The tissues collected from the sacrificed animals in the ongoing protocol were used for all experiments in this study. No treatment was administered to alter any immune cell populations.

Anesthesia and Surgery

Surgery was performed on each swine model for the creation of AVF. The minipigs were first given a preanesthetic injection of 2.5-5 mg/kg Telazol (combination of tiletamine and zolazepam) and 1-2 mg/kg xylazine SQ. Once the pigs were sedated, they were moved to the operating room and intubated for surgery. Anesthesia was maintained with isoflurane in oxygen with mechanical ventilation. IV lactated ringer solution was administered via an indwelling catheter in the ear vein. The AVF was surgically created between the femoral artery and femoral vein. The femoral artery and vein were briefly exposed and skeletonized, and all vein tributaries were ligated. Preparation for side-to-side anastomoses of the artery and vein was performed with a 1 cm incision on the medial side of the femoral artery

and lateral side of the femoral vein. The artery and vein were then anastomosed using a 6-0 proline suture. Before completing the full anastomosis, the experimental or control solution was injected into the fistula. The anastomosis was completed after 3 minutes of wait time allowing full absorption of the solution into the AVF site. After ligation was fully complete, the AVF patency was assessed by visual inspection for dilation and/or pulsation of the vein. The contralateral artery (CA) and contralateral vein (CV) were kept unaltered and used as biological control. Once the surgery was complete, the animal received prophylactic antibiotics (cefazolin 1g IM) and buprenorphine for pain. Recovery parameters were monitored until the animal was standing in their stall.

Tissue harvesting

The treatment protocol lasted for 12 weeks. After 12 weeks, AVF flow and vessel lumen were assessed using ultrasound (USG), angiography, and optical coherence tomography (OCT). The tissues collected after euthanasia were used in this study. Samples collected were proximal femoral artery (PA), and proximal femoral vein (PV), proximal to the AVF, on the experimental side. Contralateral femoral artery (CA) and contralateral femoral vein (CV) were collected as biological controls as these arteries were not surgically manipulated. Samples were fixed in 4% formalin and processed in a tissue processor. Tissue was also collected for RT-PCR in RNA-later. For tissue processing, collected tissues were treated with rounds of ethanol (70%, 90%, and 100%) for dehydration and xylazine. Tissue blocks were then made from the processed tissue using paraffin wax. These paraffin wax blocks were sectioned at 5μm using a tungsten carbide knife in a Leica RM2265 rotary microtome (LeicaTM, Germany) and attached to slides. Sectioned tissue pieces were heat blocked for 60 minutes and later used for histology and immunostaining.

Immunohistochemistry

The peroxidase anti-peroxidase method was used to perform Immunohistochemistry (IHC) using a secondary antibody conjugated to horseradish peroxidase (HRP). Tissue sections that were saved using paraffin were deparaffinized, rehydrated and antigen retrieval was performed using 1% citrate buffer (Sigma Aldrich #C9999). The slides were washed and placed in phosphate-buffered saline (PBS). The slides were dried and encircled with wax using Pep Pen. Tissue samples were then incubated with 3% hydrogen peroxide (Sigma Aldrich #H1009) for 15 minutes and then washed with PBS for 5 minutes 3 times to prepare for the blocking process. Blocking was performed using a blocking solution from the Vectastain Elite ABC kit (Vector Labs) corresponding to the primary antibody and the tissues were incubated for 1 hour at room temperature. The blocking solution was tipped off and the slides were incubated overnight at 4°C with the primary antibody. For macrophage primary antibodies, CD68 (ab955, 1:200 dilution), CD206 (ab125028, 1:200 dilution), CD86 (ab269587, 1:100 dilution), and CCR7 (ab32527, 1:100 dilution) were used to detect expression through IHC staining. For dendritic cells (DCs), primary antibodies for fascin (M3567 DAKO, 1:50 dilution) and HLA-DR (sc-73366, 1:50 dilution) were used to detect expression through IHC. For Tregs, primary antibodies for FoxP3 (ab20034, 1:100 dilution) and CD3e (ab5690, 1:50 dilution) were used to detect expression through IHC staining. The dilution of the antibody solution used was decided based on the titration of the antibodies and the dilution giving the best result was used for the final experiments. After the overnight

incubation, the slides were washed 3 times for 5 minutes each using 1x PBS solution and then incubated with the secondary antibody from the corresponding Vectastain Elite ABC kit for 1 hour at room temperature. The slides were rinsed 3 times with 1x PBS, followed by incubation with the Vectastain ABC horseradish peroxidase (HRP) for 30 minutes at room temp. The tissue sections were then rinsed with 1x PBS followed by incubation with 3,3′-diaminobenzidine (DAB) (Thermo Scientific, Cat # 34002) for 2-5 minutes until the development of the brown color of the DAB. Tissue sections were washed with water once and then stained with hematoxylin for 20-30 seconds. The slides were rinsed in running tap water for 5 minutes and mounted with a xylene-based mounting medium after air-drying the slides. The stained slides were imaged with a Leica DM6 microscope at a scale of 100 μm. The high magnification images from each tissue section were manually analyzed for average stained intensity using Fiji Image J. A minimum of three sections for each swine were used for statistical analysis.

Real-Time Quantitative Polymerase Chain Reaction (RT-qPCR)

Total RNA was extracted from collected tissues using TRIZOL method (Sigma #T9424) and the yield of RNA was measured with NanoDrop2000 (Thermo Scientific). cDNA was prepared using iSCRIPT cDNA synthesis kit (BioRad #1708891) using the manufacturer's instructions. RT-qPCR was conducted with 5-minute cycling at 95°C for initial denaturation, 40 cycles of 30s at 95°C (denaturation), 30s at 55-60°C based on primer annealing temperatures, and 30s cycle was conducted at 72°C (extension) followed by melting curve analysis in triplicate using SYBR Green Master Mix and a Real-Time PCR system (CFX, BioRad Laboratories, Hercules, CA, USA). After normalizing with 18S housekeeping gene, the fold changes in mRNA expression were calculated using the $2^{-\wedge\wedge CT}$ method. The primers used in this study were purchased from Integrated DNA Technology (IDT) and nucleotide sequences are listed in table 1.

Bioinformatics analysis

The differentially expressed genes (DEGs) related to immune cells and inflammation were selected from the RNA sequencing data (Table 2, Supplementary Table 1) and network analysis was done using Signor regulatory network analysis (networkanalyst. ca) with the list of selected DEGs as input gene list. The detailed procedure of RNA sequencing and data analysis has been described in our recent publications [6,7].

Statistical analysis

ata are presented as the mean ± SEM. Data were analyzed using GraphPad Prism 9. The comparison between two groups for the expression of the protein of interest was performed using One-way ANOVA with Bonferroni's post-hoc correction. A probability (p) value of < 0.05 was accepted as statistically significant (*p <0.05, **p<0.01, ***p <0.001 and ****p <0.0001).

Results

Gene regulatory network analysis revealed the association of differentially expressed genes with inflammation and immune response

The gene regulatory network analysis of the DEGs (Table 2) regulating immune cells from our previous study revealed the association of the input genes (Table 2) with other genes involved in inflammation, immune response, angiogenesis, adipogenesis, granulocytes differentiation, macrophage polarization, and immune cell activation (Figure 1). Further, the interaction of various chemokines, chemokine ligands, and cytokines (CCR4, CCR2, CCL2, IL-18, IL-18R, IL-15, and IFN-γ), cytoplasmic kinases (MEK1/2, ERK1/2, STATs, MAPK, and NF-κB), S100 proteins (S100A9), caspase complexes, and genes related to oxidative stress (HIF1A) and acute inflammation (CRP) with each other (Figure 1) support the role of inflammation and immune response in imparting early thrombosis and stenosis to the vessel involved in AVF and role of immune response in AVF maturation process. Furthermore, the association of DEGs with microRNAs (miR-27b, miR-27a, miR-130a) and histone deacetylases (HDACs) suggests the epigenetic regulation of the AVF maturation process (Figure 1).

AVF tissues showed higher immunopositivity of macrophages compared to contralateral arteries

Immunostaining of the AVF and controlled tissues revealed positive expression for macrophages (CD68), M1 macrophage (CCR7), and M2 macrophage (CD206). Immunostaining for CD68 was significantly higher in the AVF artery compared with the contralateral femoral artery (CA) for the LR12 peptide-treated group. Swine treated with SP had overall lower immunostaining in AVF artery and CA compared to the LR12 peptide treated group. The AVF artery in the SP group showed greater staining than CA. The contralateral femoral vein (CV) showed higher immunostaining for CD68 compared to the AVF vein in LR12 treated groups. AVF vein and CV had a similar expression for CD68 in the SP group. In the AVF artery, immunostaining was higher for the group treated with LR12 compared to the group treated with SP. AVF vein showed similar CD68 expression, with higher expression in the LR12 group compared to the SP group (Figure 2). In CCR7 stained tissue, there was higher immunopositivity in AVF artery compared to CA in swine treated with LR12 peptide while SP treated group showed higher staining for CCR7 in CA compared to AVF artery. There was no significant difference in the expression pattern between the LR12 peptide and SC peptide-treated group. CV had higher immunostaining for CCR7 compared to AVF vein in LR12 treated group. SC peptide treated group showed higher staining for CCR7 in AVF vein compared to CV. In the AVF artery, there was higher immunopositivity for the LR12 peptide treated group compared to SC treated group. In the AVF vein, there was higher immunopositivity for the SC peptide treated group compared to the LR12 peptide treated group (Figure 3). AVF artery showed higher immunostaining for CD206 compared to CA in the LR12 peptide treated group. In SP treated group, the immunostaining pattern for CD206 was higher in AVF artery compared to CA but was not significant. CV showed higher immunopositivity for CD206 compared to AVF vein in the LR12 peptide-treated group. The CV had slightly higher immunopositivity for CD206 compared to the AVF vein in the SP group. In the AVF artery, immunostaining

for CD206 showed higher staining intensity for the LR12 peptide treated group compared to the SC group. Immunostaining for CD206 was higher in the LR12 peptide group compared to the SC group in the AVF vein as well (Figure 4). The findings of increased expression of macrophages in AVF arteries and vein in LR12 and SC peptide treated group was also supported by the immunohistochemistry of ethanol and ethanol + TAK-242 treated group where Macrophages (CD68+; Supplementary Figure 1), M1 macrophages (CD86+; Supplementary Figure 2), and M2 macrophage (CD206+; Supplementary Figure 3) immunopositivity was higher in AVF vessels compared to contralateral vessels. It was also revealed that TAK-242 treatment attenuated the macrophage's density compared to ethanol treatment alone.

Dendritic cells (DCs) were shown to have higher immunopositivity in the AVF artery compared to CA

There was no significant difference in the immunopositivity for HLA-DR in AVF artery compared to CA for LR12 peptide treated group, however, SP treated group showed significantly higher immunostaining in AVF artery compared to CA for dendritic cells (HLA-DR + cells). The immunostaining for HLA-DR in AVF vein and CV was similar in both LR12 and Sc-peptide treated group and results showed no significant differences (Figure 5). Similarly, the immunopositivity for the markers for dendritic cells namely HLA-DR (Supplementary Figure 4) and Fascin (Supplementary Figure 5) was higher in AVF vessels in the ethanol and TAK-242 treated group. The immunopositivity for HLA-DR and Fascin was higher in the ethanol alone treated group compared to the ethanol + TAK242 treated group.

T-Regulatory cells (Tregs) and T-cells showed higher immunopositivity in AVF tissues compared to control vessels

AVF vein in swine treated with SC peptide showed significantly higher immunostaining for T cells (CD3e) compared to CV while in LR12 treated swine, AVF vein compared to CV showed higher stained intensity however, it was not significant. The AVF artery and CA showed similar immunopositivity for CD3e in swine treated with LR12 peptide (Figure 6). The immunostaining showed higher immunopositivity for Tregs (FoxP3) in AVF artery and vein compared to control artery and vein in LR12 peptide treated group compared to scrambled peptide treated group. AVF artery showed significantly higher immunopositivity for Tregs compared to CA in LR12 peptide treated group while the immunopositivity for Tregs in SP treated group was higher in AVF artery compared to CV but was not significant. CV showed higher immunopositivity for Tregs compared to AVF vein in LR12 peptide treated group while in SP treated group AVF vein showed slightly higher but not significant stained intensity for Tregs compared to CV (Figure 7). In the ethanol and ethanol+TAK-242 group, T cells and Treg cells' immunopositivity was higher in AVF vessels compared to contralateral femoral vessels (Supplementary Figures 6 and 7).

Increased mRNA expression for immune cells was seen across all tissue in the AVF artery treated with LR12

The folds change in mRNA expression was significantly higher in AVF arteries treated with LR12 peptide for CD68, CD86, CD206, CD163, IL-10, and CD11B compared to

contralateral control arteries. The femoral vessels treated with LR12 peptide and SP revealed significantly increased mRNA expression of CD68 in AVF artery (ProxFA) compared to CA (ContFA) in the LR12 treated peptide treated group whereas the mRNA expression for CD68 in PFA was higher but not significant compared to CA in SP treated group (Figure 8). mRNA expression in AVF vein (ProxFV) was higher than a CV in the LR12 peptide treated group while AVF vein (ProxFV) and CV had similar mRNA expression for CD68 in SP treated groups (Figure 8). RT-PCR of the vessels for CD86 showed significantly higher mRNA expression in AVF artery (ProxFA) for LR12 peptide treated group compared to CA while mRNA expression for AVF artery (ProxFA) was higher than CA in SP treated group, but it was not significant. The fold changes in mRNA expression in AVF vein (ProxFV) were higher in LR12 and SP treated group compared to the CV, but these were not significant. RT-PCR of the vessels for CD206 showed significantly higher folds change in mRNA expression in AVF artery (ProxFA) for LR12 peptide treated group compared to CA and folds change in mRNA expression for CD206 in AVF artery (ProxFA) was significantly higher than CA in SP treated group. AVF vein (ProxFV) showed higher mRNA expression in LR12, and SP treated group compared to CV but these were not significant. RT-PCR for CD163 showed significantly higher mRNA expression in AVF artery (ProxFA) and AVF vein (ProxFV) compared to CA and CV treated with LR12 and SP treated group and the folds change in mRNA expression was more in arteries compared to veins in both groups. Similarly the folds changes in mRNA expression for IL-10 were significantly higher in AVF artery (ProxFA) and AVF vein (ProxFV) compared to CA and CV treated with LR12 and SP treated group and the folds change in mRNA expression was more in arteries compared to veins in both groups (Figure 8). RT-PCR for CD11b showed significantly higher mRNA expression in AVF artery (ProxFA) compared to CA in LR12 and SP treated group while mRNA expression in AVF vein (ProxFV) compared to CV was significantly higher in SP treated group and higher but not significant in LR12 peptide treated group (Figure 8).

Discussion

This study aimed to examine the role of immune cells in AVF maturation and maturation failure because immune cells play a critical role in vascular stenosis and thrombosis [15-17]. Thus, we investigated the expression profile of genes in bulk RNA sequencing done for the ongoing project. The appearance of various differentially expressed genes (DEGs) associated with regulation, proliferation, infiltration, and activation of DCs, macrophages, Tregs, and T cells (Table 2 and Supplementary Table 1) in our sequencing data with $\log_2$fold>2 and probability (p) value <0.05 suggests the role of immune cells in early thrombosis, stenosis, and occlusion of femoral vessels and thus, maturation failure of AVF. This notion was further supported by the association of these DEGs with the differentiation of basophils, monocytes, granulocytes, mast cells, M2 polarization, M1 polarization, T-cell activation, and macrophage activation (Figure 1). Additionally, the association of these DEGs with other genes associated with inflammation including cytoplasmic kinases (ERK1/2, MAPK, MEK1/3), S100A9, HIF-1α, and regulating genetic and epigenetic (Figure 1) expression of DEGs associated with immune cells in this study (Table 2) strongly suggest the critical role of immune cells in AVF maturation and maturation failure. The results of this study were supported by the findings of bulk RNA sequencing showing

the differentially expressed genes regulating M2 macrophage polarization, monocyte differentiation, macrophage activation, M1 macrophage polarization, T cell activation, and inflammation [6,7].

We previously reported that immune response and immune cells are involved in the regulation of early thrombosis and stenosis after AVF creation [6-8]. To further evaluate the AVF tissues for immune response and the presence of immune cells, we immunostained AVF arteries and veins for immune cells. The results showed the presence of macrophages and other immune cells including dendritic cells (DCs), T-regulatory cells (Tregs), and T-cells in the femoral artery and vein involved in AVF and contralateral control femoral vessels with a higher expression profile in AVF vessels. Macrophages are pro-inflammatory cells recruited at the site of injury and help in attenuating inflammation by clearing out debris. The increased presence of macrophages in AVF tissues suggests macrophage infiltration due to intimal injury caused during AVF creation [18,19]. The two phenotypes of macrophages are pro- and anti-inflammatory macrophages. Macrophages play a critical role in three phases of inflammation. M1 predominates in the inflammatory phase while M2 predominates in the resolution phase. CD68 (M1) macrophages are present during early inflammation and have a pro-inflammatory role to clear the debris. CD206 (M2) macrophages are anti-inflammatory macrophages and play a role in the resolution of inflammation [20]. In this study, immunostaining and RT-PCR revealed increased expression of macrophages, M1 macrophages, and M2 macrophages in AVF artery and vein and the expression of macrophages was prominently in intima and adventitia. The expression of M1 macrophages higher than M2 macrophages indicate persistent inflammation which in turn is associated with plaque formation and vessel thrombosis and stenosis [21-23]. This persistent early inflammatory response may lead to early thrombosis. Additionally, the results showed the presence of macrophages in the adventitia and indicate the role of adventitial inflammation in early thrombosis [6]. Macrophages appear ubiquitously during an inflammatory response to clear debris and orchestrate other immune cells. We compared the expression of two macrophage markers, each existing on the opposite spectrum of macrophage polarity.

Progressive thickening of the intima after AVF formation led to increased hypoxia and production of reactive oxygen species (ROS). This inflammatory process leads to the recruitment and trafficking of more macrophages to the site of the lesion. Increased macrophage trafficking causes positive feedback which leads to intimal hyperplasia and neovascularization [22]. Early thrombosis of the vessel provides progressive intimal thickening and occlusion of the blood vessel. However, the immune response of the body increases M2 macrophages to attenuate inflammation and tissue repair [24]. The presence of M2 (CD206) macrophage in AVF tissues higher than in contralateral artery on immunostaining and RT-PCR suggests the immune response of the body. However, persistent inflammation due to the presence of M1 macrophages might have resulted in thrombosis and stenosis, and thus, targeting M1:M2 macrophages polarization may have therapeutic potential [25]. CD206 anti-inflammatory macrophage produces interleukin (IL)-10 and transforming growth factor (TGF)-β as their main anti-inflammatory mediators. IL-10 has been shown to decrease pro-inflammatory mediators such as MCP-1, growth factors, NF-kB, and more [25,26]. Attenuation of these markers suppresses injury response

and increases the mobilization of M2 macrophages in early lesion development, providing a promising therapeutic for AVF maturation.

Increased expression of TREM-1 on dendritic cells is associated with unstable plaque and this suggests that dendritic cells' phenotype and population may play a crucial role in plaque stability and vulnerability [13,27]. The dendritic cells (HLA-DR+ DCs) expression in AVF artery and vein was higher in scrambled treated peptide compared to contralateral artery but immunopositivity was nearly similar in AVF artery and vein in LR12 peptide treated group. This might be due to the treatment given to the swine. This notion is supported by the fact that increased HLA-DR expression is linked with high TREM-1 expression. The dendritic cell expression was higher in the AVF artery compared to the contralateral artery and dendritic cell expression (HLA-DR and Fascin+ cells) in AVF femoral cells was lower in the ethanol+TAK-242 treatment group compared to the ethanol-treated group. This suggests the effect of the treatment given to swine. Attenuated expression of DCs decreases inflammation and this might be beneficial for the patency of femoral vessels involved in AVF. Decreased expression of Facin+ DCs seen across all treated tissue indicates maturity and progression of the atherosclerotic lesion. Facin is a ubiquitous surface molecule for DC and low Facin+ shows decreased DC trafficking in mature lesion/thrombosis [28]. Also, an increase in TREM-1 via HLA-DR expression has been found associated with the inflammatory process of thrombus formation [27]. Reducing expression of HLA-DR, which also subsequently attenuates TREM-1 expression, functions in reducing the expression of CD83 and CD86 and serving as a multi-factorial anti-inflammatory therapeutic mechanism targeted for DCs in AVF development [29].

T-regulatory cells (Tregs) are important players during ischemic-reperfusion injury and ECM remodeling and interruption of vasa-vasorum and ECM remodeling occurs during AVF creation and vessel remodeling [30]. Tregs play an anti-inflammatory role and chronicity of inflammation leads to increased expression of Tregs across all tissues as an immune response of the body [31]. The presence of Tregs in the endothelium promotes vascular remodeling using inhibitory cytokines during late atherosclerotic lesions. At this point of the healing process, Tregs play a role in immunomodulation while suppressing inflammatory cells and encouraging immuno-plasticity towards anti-inflammatory cells [32]. This protective function of Tregs progresses AVF maturation and can be utilized early in therapy to prevent early thrombosis and occlusion of the blood vessel. Foxp3 decreases in number and function due to increased progression of atherosclerotic lesions [33]. Proinflammatory cytokine secretion by T-helper type-1 cells during the inflammatory phase derives an autoimmune atherosclerotic response by the immune system [34]. Presentation of antigens via APCs through MCH-II complex to T cells primes them for activation and differentiation to CD4+ effector T cells. Secretion of IFN-γ from these effector T cells promotes increased trafficking of inflammatory T cells and macrophages that promote increased atherosclerotic lesions and tissue deposition. Downstream effects of IFN-γ have been modulated by genetic deletion of IFN-γ which has been shown to markedly reduce atherosclerotic lesions in mice [34]. In our results, expression of cytotoxic CD3e was highly expressed across all AVF tissue promoting an active inflammatory response. Expression of CD3e was high across all AVF tissue samples. Downregulation of IFN-γ disrupts activation of cytotoxic T cells and Th1 cells in the group treated with LR12 compared to

the SP group. Proatherogenic compounds such as IL-6, IFN-γ, and granulocyte-macrophage colony-stimulating factors (GM-CSF) are downregulated, antagonize lesion progression, and prevent thrombosis and stenosis of vessels. During early atherosclerosis lesion progression, the regulatory/effector T-cell ratio is reduced and causes increased inflammatory response via effector T-cells. Modulation of autoimmunity via the promotion of Tregs plays a critical role in the development of atherosclerosis. Suppressing immune response mediated by effector T cells and B cells show secretion of inhibitory cytokines which inhibit macrophage inflammation and modulate cholesterol metabolism to prevent foam cell formation [35]. TLR signaling is mediated by Tregs and shows essential suppression of atherosclerosis and vascular stenosis. Early immunomodulation via Tregs helps suppress the inflammatory and tissue deposition response of macrophages to promote a pro-resolving and efferocytosis process [36]. Overall success by early immunomodulation of Tregs promotes increased wound healing and decreases inflammatory mechanisms that promote thrombosis and stenosis of AVF which produce poor AVF practicality.

Overall, the results of network analysis, immunostaining, and RT-PCR showed positive expression of immune cells including macrophages, dendritic cells, T cells, and Treg cells in the AVF tissue compared to contralateral femoral vessels suggesting the role of immune cells in AVF maturation and maturation failure [37]. Additionally, the presence of immune cells in the adventitia of the vessels suggests the ongoing pathology in the adventitia along with intima and media in stenosis, thrombosis, and vascular remodeling [6]. Thus, targeting the immune response to modulate it towards favorable vascular remodeling might be of therapeutic significance.

Conclusion

The results of the study elucidated several significant early inflammatory markers leading to early thrombosis and vessel occlusion. Targeting inflammatory immune cells associated with chronic inflammation may have had the therapeutic potential for AVF maturation, Further, the presence of immune cells in adventitia indicating immune trafficking to tunica media and tunica adventitia is another perspective of this study to target chronic inflammation and aid AVF maturation. A comparison of AVF tissue with control tissue revealed a higher immune presence in AVF tissue, even with LR12 peptide and TAK-242 treatment further suggesting the role of other mediators involved in chronic inflammation, thrombosis, and stenosis of the vessels involved in AVF. Focusing treatment on surrounding tissue and combining other treatment options may reveal promising results for attenuation of inflammation, perivascular cuffing, and early thrombosis. Additionally, the research should also be focused on the transcriptional and epigenetic regulation of AVF maturation.

Study limitations and future direction

The results of this study revealed the differential presence of immune cells in AVF vessels as well as in contralateral femoral vessels which might be due to the systemic response after AVF creation. These findings are of significance emphasizing the role of immune response and involvement of immune cells in AVF maturation and maturation failure. However, a fewer number of animals is a limiting factor and future studies are warranted

with an increased sample size. Further, no treatment was given to modulate immune cell infiltration; future studies should be conducted to further investigate the immune cell role in AVF maturation. Additionally, we performed the immunostaining and RT-PCR on collected tissues. However, these findings should be confirmed by flow cytometric analysis to quantify percent population of each immune cell in freshly collected tissues. Moreover, the percent population in tissues should be compared with the percent population in the blood to investigate the systemic response and compare with the response in AVF tissues.

Supplementary Material

Refer to Web version on PubMed Central for supplementary material.

Acknowledgement

The authors would like to thank Dr. Mohamed M. Radwan who performed the surgeries for AVF creation and helped in harvesting tissue.

Funding Support

This work was supported by the research grants R01 HL144125 and R01HL147662 to DKA from the National Heart, Lung, and Blood Institute, National Institutes of Health, USA. The contents of this chapter are solely the responsibility of the authors and do not necessarily represent the official views of the National Institutes of Health.

Data availability

Data has been provided as supplementary files and the data with the raw counts matrices and annotation are available upon request from the authors through proper channels. The complete gene list from bulk RNA seq has been uploaded at NCBI SRA (https://www.ncbi.nlm.nih.gov/sra with submission # SUB11379495.

References

1. Bevc S, Hojs R, Ekart R, Hojs-Fabjan T. Atherosclerosis in hemodialysis patients: traditional and nontraditional risk factors. Acta Dermatovenerol Alp Pannonica Adriat 15 (2006): 151–157. [PubMed: 17982607]
2. Tunbridge MJ, Jardine AG. Atherosclerotic Vascular Disease Associated with Chronic Kidney Disease. Cardiol Clin 39 (2021): 403–414. [PubMed: 34247753]
3. Bashar K, Conlon PJ, Kheirelseid EA, et al. Arteriovenous fistula in dialysis patients: Factors implicated in early and late AVF maturation failure. Surgeon 14 (2016): 294–300. [PubMed: 26988630]
4. Siddiqui MA, Ashraff S, Carline T. Maturation of arteriovenous fistula: Analysis of key factors. Kidney Res Clin Pract 36 (2017): 318–328. [PubMed: 29285424]
5. Tellides G, Pober JS. Inflammatory and immune responses in the arterial media. Circ Res 116 (2015): 312–322. [PubMed: 25593276]
6. Rai V, Agrawal DK. Transcriptomic Analysis identifies differentially expressed genes associated with vascular cuffing and chronic inflammation mediating early thrombosis in arteriovenous fistula. Biomedicines 10 (2022): 15–18.
7. Rai V, Agrawal DK. Transcriptional and Epigenetic Factors Associated with Early Thrombosis of Femoral Artery Involved in Arteriovenous Fistula. Proteomes 10 (2022): 19–25. [PubMed: 35736799]
8. Samra G, Rai V, Agrawal DK. Innate and Adaptive Immune Cells Associates with Arteriovenous Fistula Maturation and Failure. Can J Physiol Pharmacol 11 (2022) 12–15.

9. Albany CJ, Trevelin SC, Giganti G, et al. Getting to the Heart of the Matter: The Role of Regulatory T-Cells (Tregs) in Cardiovascular Disease (CVD) and Atherosclerosis. Front Immunol 10 (2019): 2795. [PubMed: 31849973]
10. Rai V, Agrawal DK. The role of damage- and pathogen-associated molecular patterns in inflammation-mediated vulnerability of atherosclerotic plaques. Can J Physiol Pharmacol 95 (2017): 1245–1253. [PubMed: 28746820]
11. Tse K, Tse H, Sidney J, et al. T cells in atherosclerosis. Int Immunol 25 (2013): 615–622. [PubMed: 24154816]
12. Lu Z, Zhang X, Li Y, et al. TLR4 antagonist reduces early-stage atherosclerosis in diabetic apolipoprotein E-deficient mice. J Endocrinol 216 (2013): 61–71. [PubMed: 23060524]
13. Rai V, Rao VH, Shao Z, et al. Dendritic Cells Expressing Triggering Receptor Expressed on Myeloid Cells-1 Correlate with Plaque Stability in Symptomatic and Asymptomatic Patients with Carotid Stenosis. PLoS One 11 (2016): e0154802. [PubMed: 27148736]
14. Rao VH, Rai V, Stoupa S, et al. Tumor necrosis factor-alpha regulates triggering receptor expressed on myeloid cells-1-dependent matrix metalloproteinases in the carotid plaques of symptomatic patients with carotid stenosis. Atherosclerosis 248 (2016): 160–169. [PubMed: 27017522]
15. Fernandez DM, Giannarelli C. Immune cell profiling in atherosclerosis: role in research and precision medicine. Nat Rev Cardiol 19 (2022): 43–58. [PubMed: 34267377]
16. McCracken IR, Taylor RS, Henderson NC, et al. Unravelling atherosclerotic heterogeneity by single cell RNA sequencing. Curr Opin Lipidol 29 (2018): 488–489. [PubMed: 30379738]
17. Wang L, Gao B, Wu M, et al. Profiles of Immune Cell Infiltration in Carotid Artery Atherosclerosis Based on Gene Expression Data. Front Immunol 12 (2021): 599–512.
18. Fan J, Watanabe T. Inflammatory reactions in the pathogenesis of atherosclerosis. J Atheroscler Thromb 10 (2003): 63–71. [PubMed: 12740479]
19. Wasse H, Huang R, Naqvi N, et al. Inflammation, oxidation and venous neointimal hyperplasia precede vascular injury from AVF creation in CKD patients. J Vasc Access 13 (2012): 168–174. [PubMed: 22020525]
20. Yang S, Yuan HQ, Hao YM, et al. Macrophage polarization in atherosclerosis. Clin Chim Acta 501 (2020): 142–146. [PubMed: 31730809]
21. Lee SG, Oh J, Bong SK, et al. Macrophage polarization and acceleration of atherosclerotic plaques in a swine model. PLoS One 13 (2018): e0193005. [PubMed: 29561847]
22. Pourcet B, Staels B. Alternative macrophages in atherosclerosis: not always protective! J Clin Invest 128 (2018): 910–912. [PubMed: 29457787]
23. Sakakura K, Nakano M, Otsuka F, et al. Pathophysiology of atherosclerosis plaque progression. Heart Lung Circ 22 (2013): 399–411. [PubMed: 23541627]
24. Stoger JL, Gijbels MJ, Manca M, et al. Distribution of macrophage polarization markers in human atherosclerosis. Atherosclerosis 225 (2012): 461–468. [PubMed: 23078881]
25. Rai V, Radwan MM, Agrawal DK. IL-33, IL-37, and Vitamin D Interaction Mediate Immunomodulation of Inflammation in Degenerating Cartilage. Antibodies (Basel) 10 (2021).
26. Zimmerman MA, Reznikov LL, Raeburn CD, et al. Interleukin-10 attenuates the response to vascular injury. J Surg Res 121 (2004): 206–213. [PubMed: 15501460]
27. Carrasco K, Boufenzer A, Jolly L, et al. TREM-1 multimerization is essential for its activation on monocytes and neutrophils. Cell Mol Immunol 16 (2019): 460–472. [PubMed: 29568119]
28. Hall MR, Yamamoto K, Protack CD, et al. Temporal regulation of venous extracellular matrix components during arteriovenous fistula maturation. J Vasc Access 16 (2015): 93–106. [PubMed: 25262757]
29. Zernecke A Dendritic cells in atherosclerosis: evidence in mice and humans. Arterioscler Thromb Vasc Biol 35 (2015): 763–770. [PubMed: 25675999]
30. Saxena A, Dobaczewski M, Rai V, et al. Regulatory T cells are recruited in the infarcted mouse myocardium and may modulate fibroblast phenotype and function. Am J Physiol Heart Circ Physiol 307 (2014): H1233–242. [PubMed: 25128167]
31. Ou HX, Guo BB, Liu Q, et al. Regulatory T cells as a new therapeutic target for atherosclerosis. Acta Pharmacol Sin 39 (2018): 1249–1258. [PubMed: 29323337]

32. Emoto T, Sasaki N, Yamashita T, et al. Regulatory/effector T-cell ratio is reduced in coronary artery disease. Circ J 78 (2014): 2935–2941. [PubMed: 25327882]

33. Foks AC, Lichtman AH, Kuiper J. Treating atherosclerosis with regulatory T cells. Arterioscler Thromb Vasc Biol 35 (2015): 280–287. [PubMed: 25414253]

34. Winkels H, Wolf D. Heterogeneity of T Cells in Atherosclerosis Defined by Single-Cell RNA-Sequencing and Cytometry by Time of Flight. Arterioscler Thromb Vasc Biol 41 (2021): 549–563. [PubMed: 33267666]

35. Xia M, Wu Q, Chen P, et al. Regulatory T Cell-Related Gene Biomarkers in the Deterioration of Atherosclerosis. Front Cardiovasc Med 8 (2021): 661–709.

36. Sharma M, Schlegel MP, Afonso MS, et al. Regulatory T Cells License Macrophage Pro-Resolving Functions During Atherosclerosis Regression. Circ Res 127 (2020): 335–353. [PubMed: 32336197]

37. Farrington CA, Cutter G, Allon M. Arteriovenous Fistula Nonmaturation: What's the Immune System Got to Do with It? Kidney 2(2021): 1743–1751.

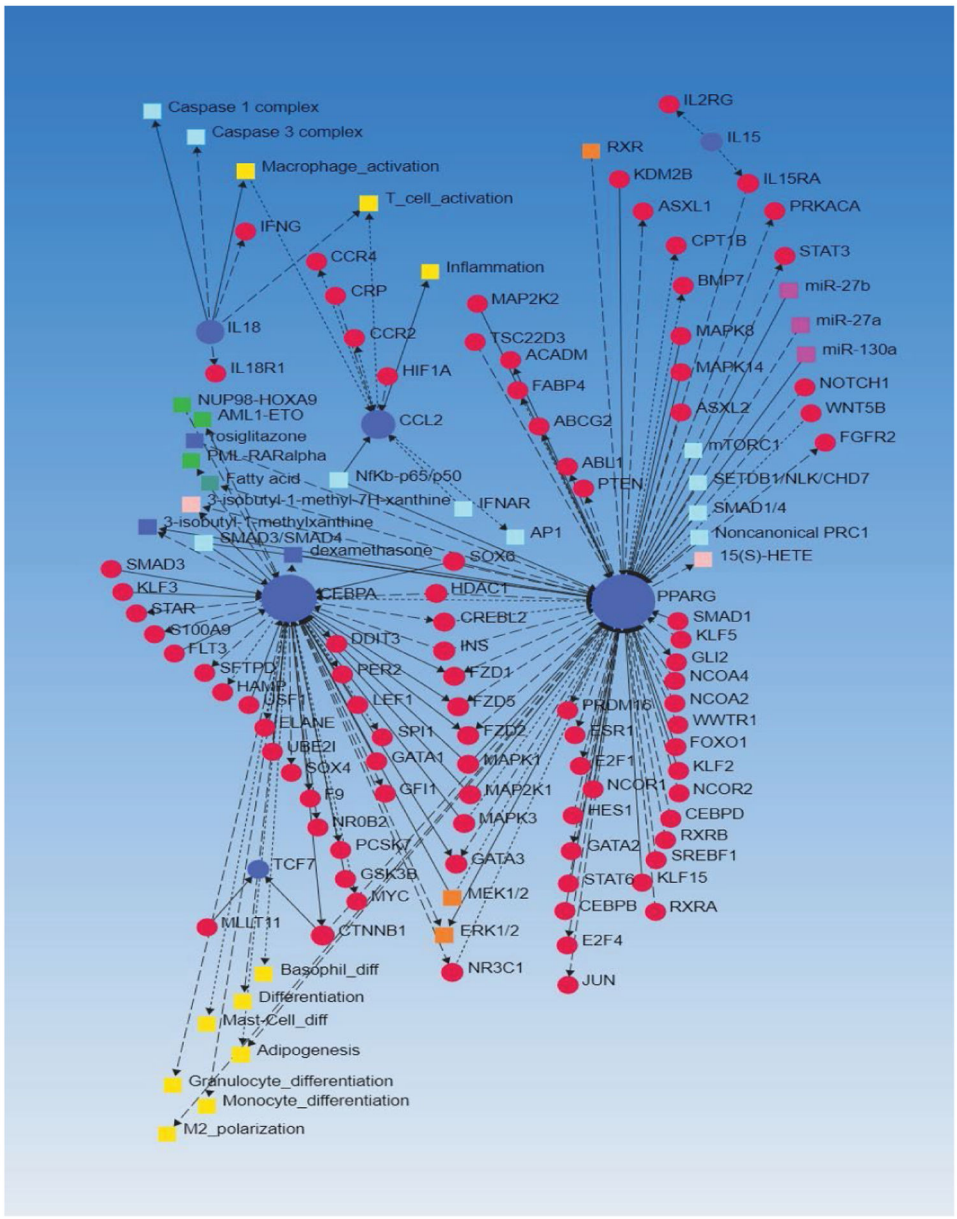

Figure 1:

Search Tool for the Retrieval of Interacting Genes/Proteins (STRING) network analysis with differentially expressed genes (DEGs) regulating immune cell development, proliferation, and migration as input genes.

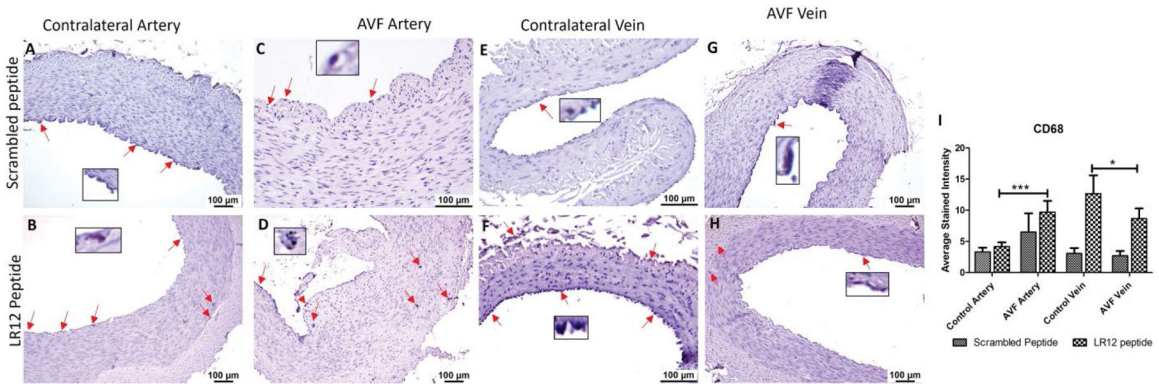

Figure 2:

Immunostaining for macrophages in femoral vessels involved in arteriovenous fistula (AVF) and contralateral femoral vessels in swine treated with triggering receptor expressed on myeloid cells (TREM)-1 inhibitor LR12 and scrambled peptide. Immunostaining for CD68 in contralateral femoral vessels (panels A, B, E, and F) and femoral vessels involved in AVF (panels C, D, G, and H), and average stained intensity (panel I). These images are represented images from all swine selected for this study. Inset shows higher magnification images of immune cells and red arrows show the positively stained immune cells. All data are presented as Mean ± SEM. A probability (p) value <0.05 was considered significant. *p<0.05, ***p<0.001.

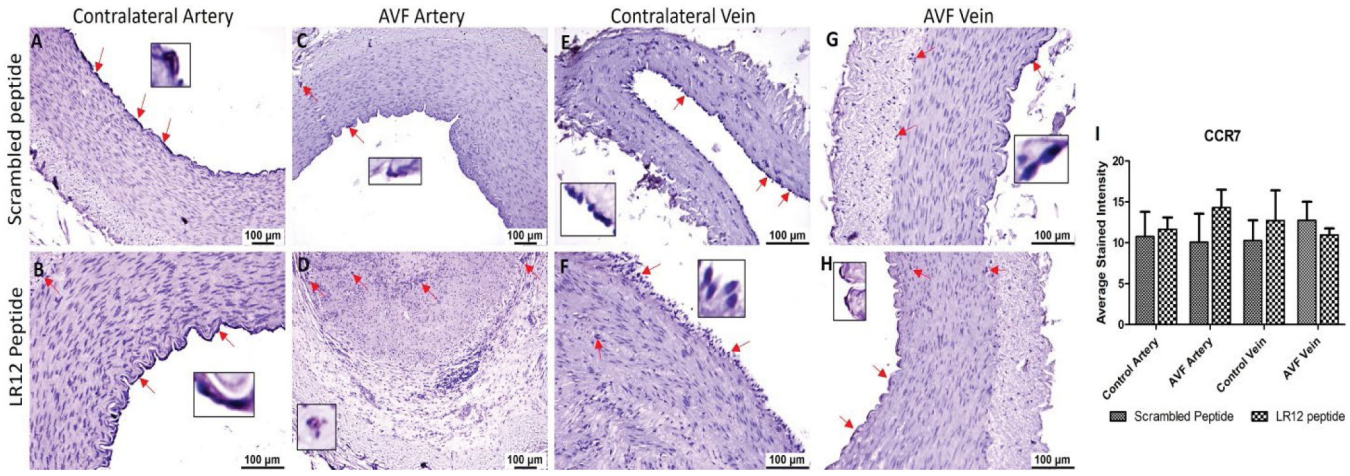

Figure 3:

Immunostaining for macrophages in femoral vessels involved in arteriovenous fistula (AVF) and contralateral femoral vessels in swine treated with triggering receptor expressed on myeloid cells (TREM)-1 inhibitor LR12 and scrambled peptide. Immunostaining for CCR7 in contralateral femoral vessels (panels A, B, E, and F) and femoral vessels involved in AVF (panels C, D, G, and H), and average stained intensity (panel I). These images are represented images from all swine selected for this study. Inset shows higher magnification images of immune cells and red arrows show the positively stained immune cells. All data are presented as Mean ± SEM.

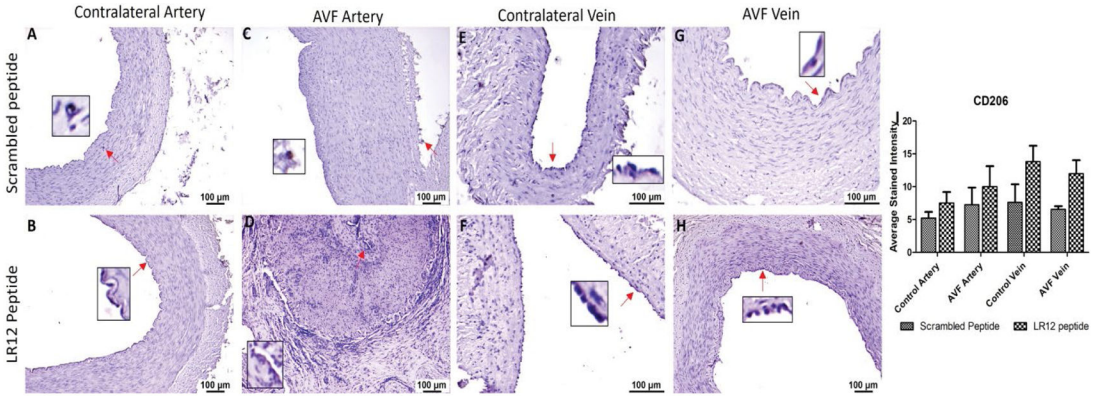

Figure 4:

Immunostaining for macrophages in femoral vessels involved in arteriovenous fistula (AVF) and contralateral femoral vessels in swine treated with triggering receptor expressed on myeloid cells (TREM)-1 inhibitor LR12 and scrambled peptide. Immunostaining for CD206 in contralateral femoral vessels (panels A, B, E, and F) and femoral vessels involved in AVF (panels C, D, G, and H), and average stained intensity (panel I). These images are represented images from all swine selected for this study. Inset shows higher magnification images of immune cells and red arrows show the positively stained immune cells. All data are presented as Mean ± SEM.

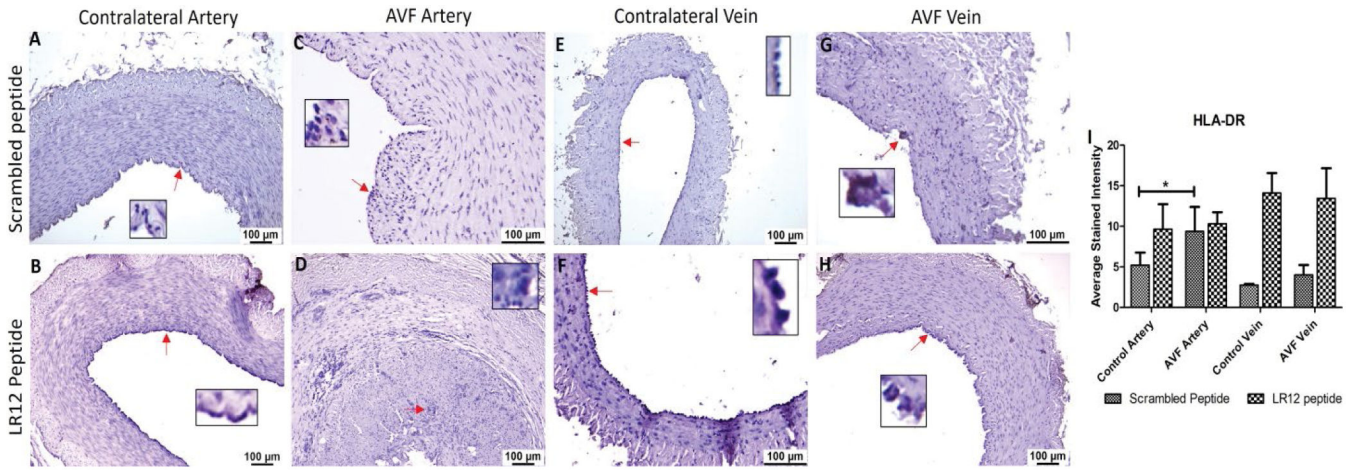

Figure 5:

Immunostaining for dendritic cells in femoral vessels involved in arteriovenous fistula (AVF) and contralateral femoral vessels in swine treated with triggering receptor expressed on myeloid cells (TREM)-1 inhibitor LR12 and scrambled peptide. Immunostaining for HLA-DR in contralateral femoral vessels (panels A, B, E, and F) and femoral vessels involved in AVF (panels C, D, G, and H), and average stained intensity (panel I). These images are represented images from all swine selected for this study. Inset shows higher magnification images of immune cells and red arrows show the positively stained immune cells. All data are presented as Mean ± SEM. A probability (p) value <0.05 was considered significant. *p<0.05.

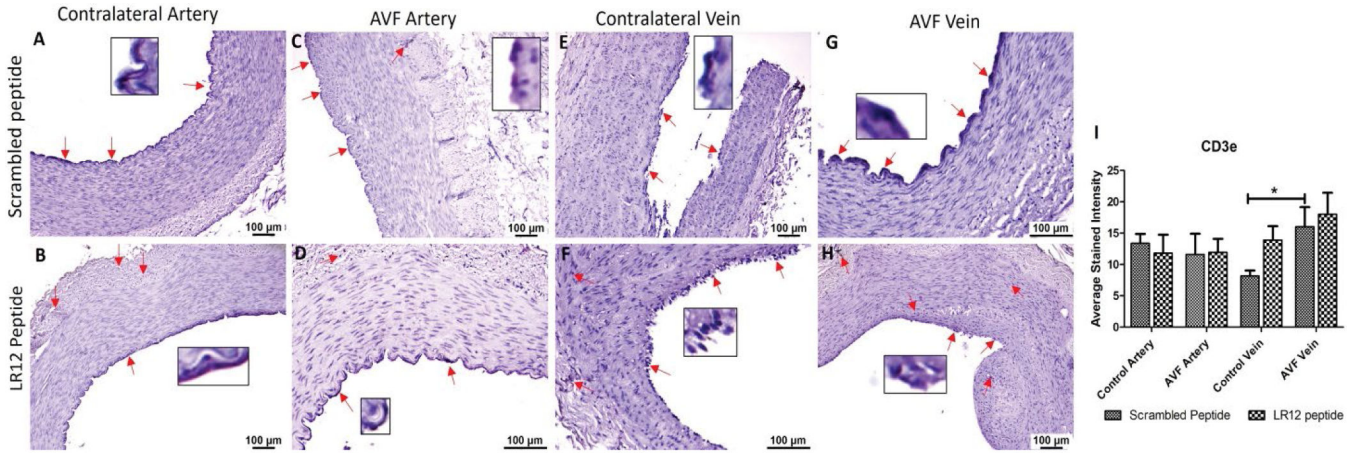

Figure 6:

Immunostaining for T lymphocytes in femoral vessels involved in arteriovenous fistula (AVF) and contralateral femoral vessels in swine treated with triggering receptor expressed on myeloid cells (TREM)-1 inhibitor LR12 and scrambled peptide. Immunostaining for CD3e in contralateral femoral vessels (panels A, B, E, and F) and femoral vessels involved in AVF (panels C, D, G, and H), and average stained intensity (panel I). These images are represented images from all swine selected for this study. Inset shows higher magnification images of immune cells and red arrows show the positively stained immune cells. All data are presented as Mean ± SEM. A probability (p) value <0.05 was considered significant. *p<0.05.

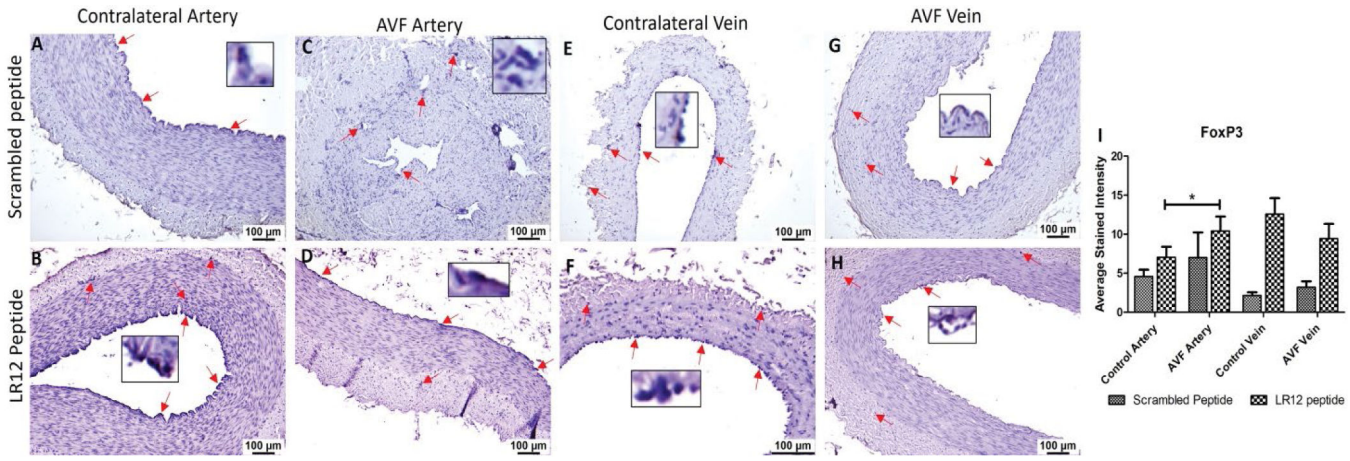

Figure 7:

Immunostaining for T-regulatory cells in femoral vessels involved in arteriovenous fistula (AVF) and contralateral femoral vessels in swine treated with triggering receptor expressed on myeloid cells (TREM)-1 inhibitor LR12 and scrambled peptide. Immunostaining for FoxP3 in contralateral femoral vessels (panels A, B, E, and F) and femoral vessels involved in AVF (panels C, D, G, and H), and average stained intensity (panel I). These images are represented images from all swine selected for this study. Inset shows higher magnification images of immune cells and red arrows show the positively stained immune cells. All data are presented as Mean ± SEM. A probability (p) value <0.05 was considered significant. *p<0.05.

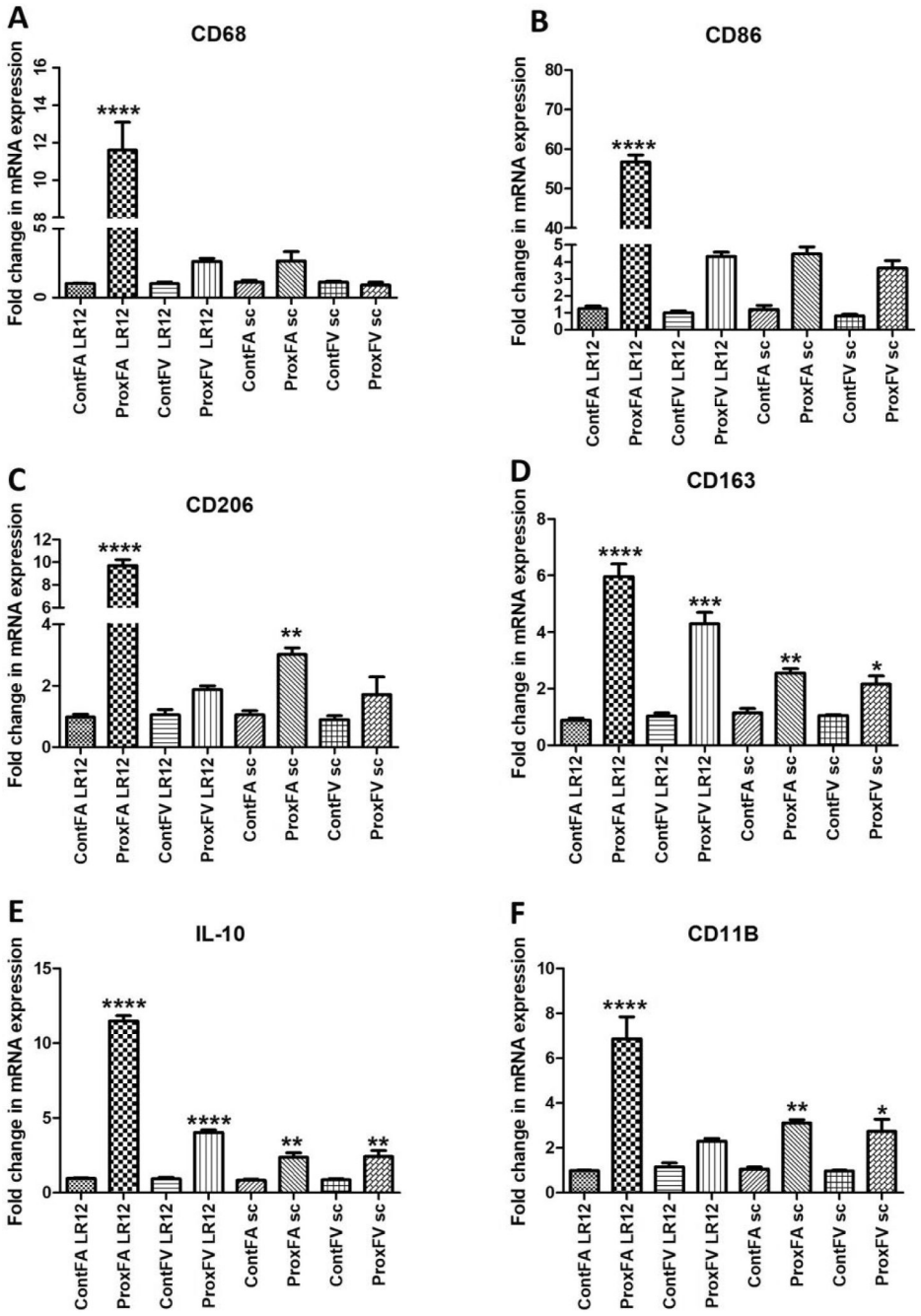

Figure 8:

RT-PCR analysis for mRNA expression of markers of immune cells. CD68 (macrophages, panel A), CD86 (M1 macrophages, panel B), CD206 (M2a macrophages, panel C), CD163 (M2b macrophages, panel D), IL-10 (M2c macrophages, panel E), and lymphocytes (CD11b, panel F). All data are presented as Mean ± SD. A probability (p) value <0.05 was considered as significant. *p<0.05, **p<0.01, ***p<0.001,****p<0.0001.

Table 1:

Nucleotide sequence of the primers used in RT-qPCR for this study

CD11b	
Forward Primer	5’-CAACTTCTCTCTGGTGGGAAAG-3’
Reverse Primer	5’-GGGAAACAAGGCTGTGAAGA-3’
CD68	
Forward Primer	5’-TCCCAGTGACCAAACCATCC-3’
Reverse Primer	5’-TTGGAACAGATGCTCACGGA-3’
CD86	
Forward Primer	5’-GTTGTGTGTGGGATGGTGTC-3’
Reverse Primer	5’-GTTTGTTCACTCGCCTTCCTG-3’
CD206	
Forward Primer	5’-TAGGGGTGCCCTCAAAAACC-3’
Reverse Primer	5’-GCGTGTCATTTCTGCACTCC-3’
CD163	
Forward Primer	5’-CTGTGATGATGGCTGGGATAG-3’
Reverse Primer	5’-AATGTGTCCAGTTCCCTCAC-3’
IL-10	
Forward Primer	5’-GCTGGAGGACTTTAAGGGTTAC-3’
Reverse Primer	5’-CTCTCTGCCTTCGGCATTAC-3’

Table 2:

Differentially expressed genes associated with immune cell regulation, proliferation, and activation.

ID	Gene name	log_2FoldChange	*p* value
ENSSSCG00000025578	ALDH1A2	2.194614	0.026455
ENSSSCG00000006452	CD1D	2.30609	0.00031
ENSSSCG00000006309	CD247	2.783942	0.000659
ENSSSCG00000017723	CCL2	2.091357	0.038906
ENSSSCG00000002821	CCL22	4.877724	0.008741
ENSSSCG00000006736	CD2	3.495897	0.010524
ENSSSCG00000000705	CD27	3.49071	0.02786
ENSSSCG00000008742	CD38	3.445621	0.040532
ENSSSCG00000015093	CD3D	4.495139	0.004869
ENSSSCG00000013115	CD5	4.014829	0.009563
ENSSSCG00000002866	CEBPA	4.051272	0.000885
ENSSSCG00000016688	CPVL	7.06123	0.040958
ENSSSCG00000016855	FYB1	2.061425	0.000838
ENSSSCG00000022490	GPR83	7.122631	0.037586
ENSSSCG00000013655	ICAM1	2.290077	0.034718
ENSSSCG00000009051	IL15	2.04075	0.00096
ENSSSCG00000015037	IL18	2.838559	1.20E-05
ENSSSCG00000011579	PPARG	4.038436	0.000948
ENSSSCG00000013839	RASAL3	3.355867	0.043788
ENSSSCG00000015550	RGS16	3.14923	0.045747
ENSSSCG00000030680	TCF7	2.736719	0.035526
ENSSSCG00000022512	TRDC	4.254936	0.007944
ENSSSCG00000029813	TSPAN5	2.098272	0.025936